Investigation of Steady Magnetohydrodynamics Casson Fluid Flow over an Aligned Vertical Porous Plate in the Presence of Thermal Radiation and Thermal Diffusion Impacts

A. Shakila[1], R. Vijayaragavan[2] and S. Karthikeyan[3,*]

[1]Research Scholar, Department of Mathematics, Thiruvalluvar University, Vellore, Tamilnadu-632115, India.
[2]Professor, Department of Mathematics, Thiruvalluvar University, Vellore, Tamilnadu-632115, India.
[3,]Assistant Professor, Department of Mathematics, Loyola College, Tiruvannamalai, Tamilnadu-606754, India.*

Abstract : *This study examines the influence of aligned angle and radiation on fluid flow in an infinite vertical plate submerged in a porous medium under steady magnetohydrodynamics (MHD) with thermal convection. The flow of a Casson fluid, representing an incompressible viscous fluid in an isotropic state, is analyzed using a physical equation. The governing partial differential equations are solved using a mathematical approach, and dimensionless equations for velocity, temperature, and concentration are derived using the perturbation technique. MATLAB-generated graphs illustrate the effects of various parameters, including Grashof number, modified Grashof number, magnetic parameter, Casson parameter, permeability parameter, aligned angle, Prandtl number, radiation parameter, heat absorption, Schmidt number, and chemical reaction. A comparative analysis with existing research is presented, including data on skin friction and Nusselt number, in a tabular format. This study's findings contribute to a better understanding of fluid dynamics in porous media and can be applied to optimize heat transfer processes in various engineering applications.*

Keywords: MHD, Casson fluid, Aligned angle, Radiation parameter and Soret effect.

1. Introduction

All the fields of industrial science, food science, engineering, and mechanics study non-Newtonian fluids. One class of Casson fluids is non-Newtonian fluids. In particular, plastic goods are produced using plastic. Additionally, petroleum and crude oil are separated using these fluids. The yield shear stress is represented by the equation of strain, which is an elastic solid. For example, non-Newtonian materials such as milk, algae, tomatoes, shampoo, paint, and blood are used.

The effect of chemical reactions on the concentration and temperature of absorption through a vertical plate with convection paste on a past magnetohydrodynamic wall [1]. Heat production and absorption in a Casson fluid flow in an infinite porous media on an unstable MHD vertical plate during radiative absorption in the presence of extremely accelerated convection [2]. Compressed flow near the sensor surface of a Maxwell fluid by penetrating radiation and chemical reactions [3]. Unsteady MHD fluid flow and radiative and soret effects of chemical reactions through a red porous plate in the presence of an obliquely oriented magnetic field [4]. Heat diffusion effects on previously unstable MHD exponentially accelerate free convective flow over a porous medium in a semi-infinite vertical plate [5]. The thermodynamic impact of thermal radiation and chemical reactions on radiative absorption and diffusion in unsteady MHD in an inclined porous plate [6]. The heat and mass transfer effects of slip in the presence of Kuvshinski fluid flow through an inclined, unstable MHD porous plate [7]. The use of diffusion thermo and heat dissipation effects on maximum well nanofluid flow through convective flow by nonlinear radiation of heat flow using MHD 3D mixing [8]. A vertical porous medium in MHD that allows free conduction via a plate at a heat source and radiation absorption [9]. The effects of a magnetic field applied in a stretching/shrinking sheet on the flow of a convected Maxwell fluid and the transmission of heat [10]. The rapid temperature change in MHD is caused by the mass distribution of a vertical plate embedded in a porous medium and the heat source's impact through a radiative absorber fluid [11]. The effects of thermal conductivity and convective flow via diffusion in a Maxwell nanofluid with MHD mixing in a porous medium with vertical cones [12]. Chemical reactions via the passage of free convective radiation in a porous vertical plate in MHD [13]. Unstable MHD, soret, and radiation effects via Guvshinski fluid flow and chemical reactions via an angled porous plate [14]. The effects of Soret and chemical reactions on fluid flow for heat transfer in the presence of irregular MHD heat and radiation absorption in an infinite vertical plate [15]. A Newtonian fluid flows through thermodynamic flow over an inclined plate in unstable MHD. Dufour effects manifest as both chemical reactions and radiative absorption [16]. The impact of radiation on chemical reactions and the Soret effect in the presence of fluid flow slip in unstable MHD systems [17]. Heat radiation and transfer effects during NHD fluid flow via a fixed vertical plate with a fixed porous medium [18–19]. Thermal radiation flows through an accelerating vertical plate with a porous medium in steady MHD in the presence of a Casson fluid flow [20]. Solutions for Casson fluid flow in unsteady free convection across an oscillating vertical plate and a wall of constant temperature [21]. The effects of a chemical reaction in an unstable MHD-free convection flow embedded in a porous material with variable absorption [22]. Heat radiation forms at the surface as a result of heat transfer in high-speed micro stretching and Casson fluid flow [23]. Radiation as occurring in the presence of an exponentially extending magnetic field in a Casson fluid paste [24]. Slip effects with convection in the presence of an upward gradient in an elastic sheet boundary layer in a fluid flow enclosed in a porous medium in MHD [25]. The analysis of an exponentially stretched sheet with a Casson fluid flow in MHD [26]. High-speed fin plates in convective solutions and thermally unstable Casson fluid flow under boundary conditions and modeling [27]. Utilizing past gas flow and a DTM numerical probe on ultrafast variable thermal radiation in a stretched sheet was constructed [28]. Chemical reactions and heat diffusion in the study of Casson fluid flow using a porous plate under the influence of MHD [29]. Thermal and radiation diffusion via a vertical porous plate in the slip flow regime of an inhomogeneous MHD fluid flow with chemical reaction [30].

This paper focuses on the aligned angle and radiation in the magnetic field, where the parameters are defined using skin friction, the Nusselt number, and the Sherwood number, and the governing equations are solved analytically using the perturbation technique to find the dimensionless equations of velocity, temperature, and concentration. Execute the aforementioned parameters in sectors that are industry-specific. As an instance, several industries, including biomechanics, polymers, manufacturing, and medicine, use this fluid.

2. Basic Equations

A magnetic field combined with an electric and incompressible viscous field can be used to find the Casson flow equation.

The continuity equation

$$\overline{\nabla}.\overline{q}=0$$

(1)

Equation of momentum

$$\rho\left[\left(\overline{q}.\overline{\nabla}\right)\overline{q}\right]=-\overline{\nabla}p+\overline{J}\cdot\overline{\mathrm{B}}+\rho\overline{g}+\mu\nabla^2\overline{q}-\left[\left|\frac{\mu}{\mathrm{K}'}\right|\right]\overline{q} \tag{2}$$

The law of Ohm

$$\overline{J}=\sigma\left[\overline{\mathrm{E}}+\left(\overline{q}\cdot\overline{\mathrm{B}}\right)\right] \tag{3}$$

The magnetism law of Gauss

$$\overline{\nabla}.\overline{\mathrm{B}}=0 \tag{4}$$

The energy formula

$$\rho C_P\left[\left(\bar{q}.\bar{\nabla}\right)T'\right]=\mathrm{K}\nabla^2T'+\mu\left(\nabla.\bar{q}\right)^2-\nabla q_r{}'+\mu\nabla^2\bar{q}^2-Q'\left(T'-T_\infty{}'\right) \tag{5}$$

Equation for the continuity of species

$$\left(\bar{q}.\bar{\nabla}\right)C'=D_M\nabla^2C'+K'\left(C_\infty{}'-C'\right)+\frac{D_M\mathrm{K}_T}{T_M}\nabla^2T' \tag{6}$$

3. Mathematical Formulation

The unstable two-dimensional model depicted in Figure.1 shows an incompressible viscous Casson nanofluid flowing across a vertical plate with a porous media. It transfers electricity through a porous material. The direction of the fluid flow's x and y axes is upward and normally, respectively. In an incline magnetic field, the fluid is moving. Its viscosity and heat conductivity are also constant. In a discontinuous magnetic field, the following formulas relate to radiation and incompressible viscous Casson fluid flow.

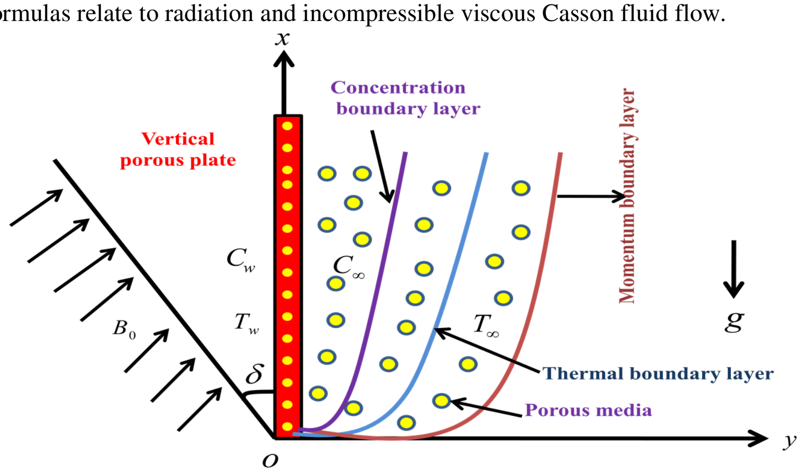

Figure 1. Physical configuration.

A physical equation can be used to express the isotropic condition in an incompressible Casson fluid flow [30],

$$\tau_{ij}=\begin{cases}\left(\mu_\beta+\frac{\mathrm{P}_y}{\sqrt{2\pi}}\right)e_{ij,}\pi>\pi_c,\\ 2\\ \left(\mu_\beta+\frac{\mathrm{P}_y}{\sqrt{2\pi_c}}\right)e_{ij,}\pi>\pi_c.\end{cases} \tag{7}$$

The decay rate (i,j) is e_{ij} and the critical value πc of this product is given in equation. (7) $\pi=e_{ij}$ is the product of the decay rate π.

In a non-Newtonian fluid, the yield stress is denoted as P_y and the plastic dynamic viscosity as μ_β.

$$\mathrm{P}_y=\frac{\mu_\beta\sqrt{2\pi}}{\gamma} \tag{8}$$

When the shear stress is needed to progressively increase during Casson fluid flow and in some fluids at a steady state, the fluid is said to be rheopectic if it is maintained at a constant yield stress to preserve the strain ratio where $\pi > \pi_c$

$$\mu = \mu_\beta + \frac{\mathrm{P}_y}{\sqrt{2\pi}} \tag{9}$$

The equation for kinematic viscosity can be obtained by substituting Equation (8) into Equation. (9).

$$\nu = \frac{\mu}{\rho} = \frac{\mu_\beta}{\rho}\left(1+\frac{1}{\gamma}\right) \tag{10}$$

Where $\gamma = \frac{\mu_\beta\sqrt{2\pi_c}}{\mathrm{P}_y}$ is the Casson parameter in the case. While $\gamma \to \infty$ is a Newtonian fluid, it conceals the nature of non-Newtonian fluid.

Using forward flow equation, Obulesu Mopuri et al. [19] determined the equations regulating conservation under the aforementioned assumptions of particular momentum, energy, concentration and mass.

$$\frac{\partial \upsilon'}{\partial y'} = 0 \tag{11}$$

$$\upsilon'\frac{\partial u'}{\partial y'} = \nu\left(1+\frac{1}{\gamma}\right)\frac{\partial^2 u'}{\partial y'^2} + g\beta_T\left(T'-T'_\infty\right) + g\beta_C\left(C'-C'_\infty\right) - \frac{\sigma B_0^2}{\rho}u'\sin^2\delta - \nu\frac{u'}{K_p} \tag{12}$$

$$\upsilon'\frac{\partial T'}{\partial y'} = \frac{\mathrm{K}}{\rho C_p}\frac{\partial^2 T'}{\partial y'^2} + \frac{\nu}{C_p}\left(1+\frac{1}{\gamma}\right)\left(\frac{\partial u'}{\partial y'}\right)^2 - \frac{1}{\rho C_p}\frac{\partial q_r'}{\partial y'} + \frac{\sigma B_0^2}{\rho C_p}u'^2 - \frac{Q_1}{\rho C_p}\left(T'-T'_\infty\right) \tag{13}$$

$$\upsilon'\frac{\partial C'}{\partial y'} = D\frac{\partial^2 C'}{\partial y'^2} - K_C\left(C'-C'_\infty\right) + D_1\frac{\partial^2 T'}{\partial y'^2} \tag{14}$$

Levels of boundary relationships

$$u'=0,\quad T'=T_W,\quad C'=C_W,\qquad at\ \ y'=0$$
$$u'\to 0,\quad T'\to 0,\quad C'\to 0\qquad at\ \ y'\to\infty$$

(15)

Equation.(11) gives the equation of continuity using a function of time or constant υ'.

$$\upsilon' = -\upsilon_0'\left(1+\varepsilon e^{n*t*}\right) \tag{16}$$

The suction velocity on the plate is denoted by $\upsilon' > 0$, a positive constant that signifies that the velocity absorbs the negative sign as it approaches the plateau.

$$\frac{\partial q_r'}{\partial y'} == 4I_1'\left(T'-T'_\infty\right) \tag{17}$$

Originally, a nondimensional scale was employed by

$$u=\frac{u'}{\upsilon_0}, \mathrm{y}=\frac{\upsilon_0 y'}{\vartheta}, \theta=\frac{(T'-T'_\infty)}{(T'_w-T'_\infty)}, \varphi=\frac{(C'-C'_\infty)}{(C'_w-C'_\infty)}, \mathrm{Pr}=\frac{\mu C_p}{K_T}, Sc=\frac{\vartheta}{D}, M=\frac{\sigma B_o^2\vartheta}{\rho\upsilon_o^2},$$
$$Gr=\frac{\vartheta g\beta_T(T'_w-T'_\infty)}{\upsilon_o^3}, Gm=\frac{\vartheta g\beta_C(C'_w-C'_\infty)}{\upsilon_o^3}, E=\frac{\upsilon_o^2}{C_p(T_w-T'_\infty)}, K=\frac{\upsilon_o^2 K_p}{\vartheta^2}, \tag{18}$$
$$K_o=\frac{\vartheta K_C}{\upsilon_o^2}, F=\frac{4I_1\vartheta^2}{K\upsilon_o^2}, Q=\frac{Q_1\upsilon^2}{K\upsilon_o^2}, \mathrm{So}=\frac{D_1(T_w-T'_\infty)}{\vartheta(C_w-C'_\infty)}, t=\frac{t'\upsilon_o^2}{4\vartheta}, h=\frac{\upsilon_o^2 L_1}{\vartheta}, R=\frac{4I'\vartheta}{\vartheta C_p\upsilon_o^2}$$

The nondimensional governing equations (11)-(14) can be used to rewrite this process in dimensional form

$$\left(1+\frac{1}{\gamma}\right)u''+u'=-Gr\theta-Gm\varphi+M_1u \tag{19}$$

$$\theta''+Pr\theta'-(F+Q)\theta=-\mathrm{Pr}\,E\left(1+\frac{1}{\gamma}\right)u'^2-\mathrm{Pr}\,EMu^2 \quad (20$$

$$\varphi''+Sc\varphi'-ScK_o\varphi=-S_0Sc\theta'' \tag{21}$$

Where $M_1=M\sin^2\delta+\dfrac{1}{K}$

Dimensional form of boundary conditions

$$\begin{aligned} &u=0,\quad T=1,\quad C=1, \qquad at\ \ y=0\\ &u\to 0,\ T\to 0,\ C\to 0 \qquad at\ \ y\to\infty \end{aligned} \tag{22}$$

4. Solution of the Problem

The velocity, temperature and concentration dimensionless forms of the ordinary differential equations (19)–(21) were solved. Additionally, it can be applied to analytically resolve partial differential equation problems in closed form, using a collection of

$$\begin{aligned} u(y,t)&=u_0(y)+\varepsilon u_1(y)e^{mt},\\ \theta(y,t)&=\theta_0(y)+\varepsilon\theta_1(y)e^{mt},\\ \phi(y,t)&=\phi_0(y)+\varepsilon\phi_1(y)e^{mt}. \end{aligned} \tag{23}$$

4.1 Zero order terms

$$\left(1+\frac{1}{\gamma}\right)u_0''+u_0'=-Gr\theta_0-Gm\varphi_0+M_1u_0 \tag{24}$$

$$\theta_0''+Pr\theta_0'-(F+Q)\theta_0=0 \tag{25}$$

$$\varphi_0''+Sc\varphi_0'-ScK_o\varphi_0=-S_0Sc\theta_0'' \tag{26}$$

4.2 First order terms

$$\left(1+\frac{1}{\gamma}\right)u_1''+u_1'=-Gr\theta_1-Gm\varphi_1+M_1u_1 \tag{27}$$

$$\theta_1''+Pr\theta_1'-(F+Q)\theta_1=-Pr\left(1+\frac{1}{\gamma}\right)u_0'^2-PrMu_0^2 \tag{28}$$

$$\varphi_1''+Sc\varphi_1'-ScK_o\varphi_1=-S_0Sc\theta_1'' \tag{29}$$

The matching limits conditions are

$$\begin{aligned}&u_0=0,\;\; u_1=0,\;\; \theta_0=1,\;\; \theta_1=0,\;\; \phi_0=1,\;\; \phi_1=0 \;\; at \;\; y=0\\ &u_0\to 0,\, u_1\to 0,\, \theta_0\to 0,\, \theta_1\to 0,\, \phi_0\to 0,\, \phi_1\to 0 \; at \;\; y\to\infty\end{aligned} \tag{30}$$

The temperature, concentration and velocity boundary conditions are given below. Equations (23)–(29) can be solved by substituting equation (30).

$$\begin{aligned}u=&Z_3e^{-w_1y}-Z_4e^{-w_2y}+Z_5e^{-w_3y}+\varepsilon[Z_{33}\,e^{-w_1y}+Z_{34}e^{-w_2y}+Z_{35}e^{-2w_1y}\\ &+Z_{36}e^{-2w_2y}+Z_{37}e^{-2w_3y}+Z_{38}e^{-\alpha_1y}+Z_{39}e^{-\alpha_2y}+Z_{40}e^{-\alpha_3y}+Z_{41}e^{-w_3y}]\end{aligned} \tag{31}$$

$$\begin{aligned}\theta=&e^{-w_1y}+\varepsilon[Z_{18}\,e^{-2w_1y}+Z_{19}e^{-2w_2y}+Z_{20}e^{-2w_3y}+Z_{21}e^{-\alpha_1y}+Z_{22}e^{-\alpha_2y}\\ &+Z_{23}e^{-\alpha_3y}+Z_{24}e^{-w_1y}]\end{aligned}$$

(32)

$$\begin{aligned}\varphi=&-Z_1e^{-w_1y}+Z_2e^{-w_2y}+\varepsilon[Z_{25}\,e^{-w_1y}+Z_{26}e^{-2w_1y}+Z_{27}e^{-2w_2y}+Z_{28}e^{-2w_3y}\\ &+Z_{29}e^{-\alpha_1y}+Z_{30}e^{-\alpha_2y}+Z_{31}e^{-\alpha_3y}+Z_{32}e^{-w_2y}]\end{aligned}$$

(33)

4.3 Skin friction

Skin friction is generated in a nondimensional form by the relation.

$$\tau=\left(\frac{\partial u}{\partial y}\right)_{y=0}$$

$$\begin{aligned}\tau=&[-w_1Z_3+w_2Z_4-w_3Z_5]+\varepsilon[\mathrm{w}_1\,Z_{33}-w_2Z_{34}-2w_1Z_{35}-2w_2Z_{36}\\ &-2w_3Z_{37}-\alpha_1Z_{38}-\alpha_2Z_{39}-\alpha_3Z_{40}-w_3Z_{41}]\end{aligned} \tag{34}$$

4.4 Rate of heat transfer

The nondimensional Nusselt number can be utilized to compute the heat transfer coefficient's rate as

$$Nu = -\left(\frac{\partial \theta}{\partial y}\right)_{y=0}$$

$$Nu = w_1 + \varepsilon[\mathrm{w}_1 Z_{24} + 2w_1 Z_{18} + 2w_2 Z_{19} + 2w_3 Z_{20} + \alpha_1 Z_{21} + \alpha_2 Z_{22} + \alpha_3 Z_{23}] \quad (35)$$

4.5 Rate of mass transfer

The mass transfer coefficient's rate can be calculated using the nondimensional Sherwood number as

$$Sh = -\left(\frac{\partial \varphi}{\partial y}\right)_{y=0}$$

$$Sh = [\mathrm{w}_2 Z_2 - w_1 Z_1] + \varepsilon[\mathrm{w}_1 Z_{25} + 2w_1 Z_{26} + 2w_2 Z_{27} + 2w_3 Z_{28} + \alpha_1 Z_{29} + \alpha_2 Z_{30} + \alpha_3 Z_{31} + w_2 Z_{32}] \quad (36)$$

5. Results and Discussion

The previously mentioned analytical results are clearly shown in the set Figure (2) – (12) by using the perturbation approach to numerically analyses the results through MATLAB. The surface heat force and the boundary layer hydrodynamic force are compared. The effects of temperature, concentration, and velocity profiles are extracted using standard physical parameters. As the vertical plate fluid absorption parameter increases, the velocity, temperature, and concentration level become visible. Charts display their parameters. The Casson fluid (γ), Grashof number (Gr), alignment angle (δ), permeability parameter (K), modified Grashof number (Gm), heat absorption (Q), radiation parameter (F), Prandtl number (Pr), Schmidt number (Sc), and chemical reaction (K_o) and the outcomes. We discuss some of the important flow properties of the model under the assumption that $\mathrm{Pr} = 7,\ \gamma = 0.5,\ M = 2,\ \delta = \frac{\pi}{3},\ Gr = 5,\ Gm = 5,$ $Sc = 0.22,\ K_0 = 1,\ S_0 = 1,\ F = 1,\ K = 1$ and $Q = 1$ are fixed.

Figure (2) indicates that the liquid absorption rate increases in tandem with an increase in the Casson parameters. The velocity of the hydrodynamic force increases in graphs (3) and (4) Gr and Gm in proportion to the increase in the thermal force parameter. Diagram (5) shows how the fluid's flow is impeded by the Lorentz force, which causes the velocity to drop as the magnetic parameter increases. The hydrodynamic force in the boundary layer causes the velocity to increase in graphs (6) and (7).

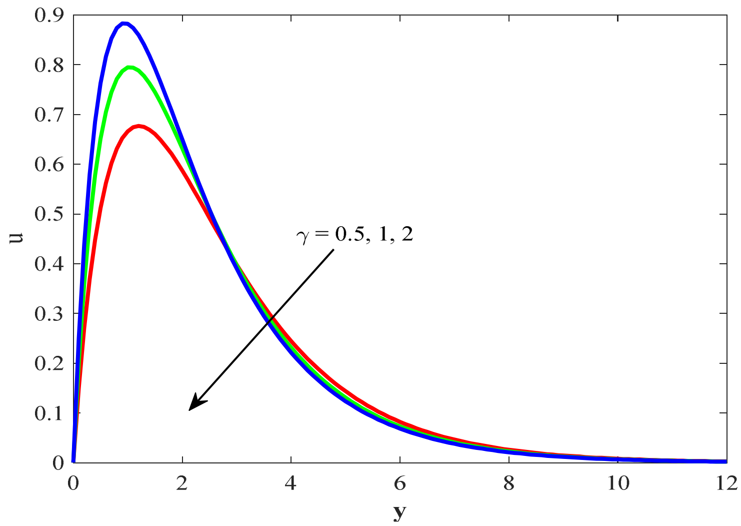

Figure 2. Impact of velocity profile at various γ values.

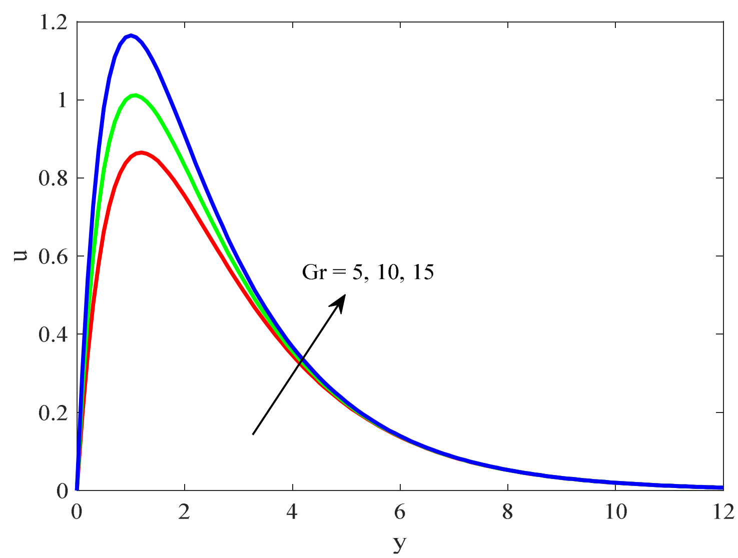

Figure 3. Impact of velocity profile at various Gr values.

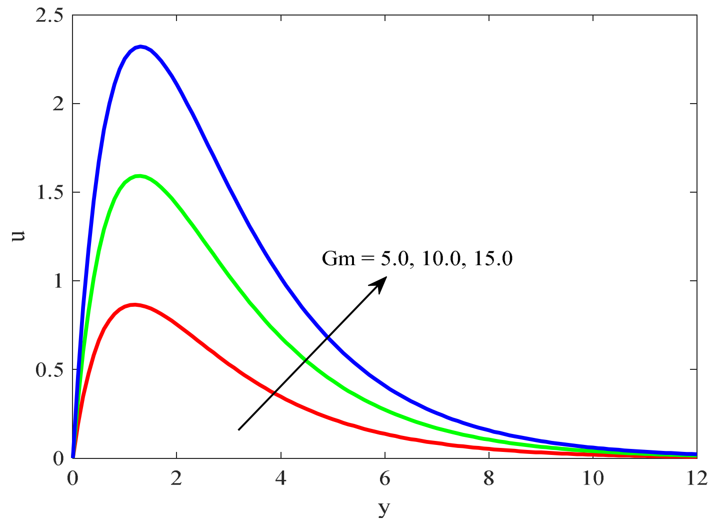

Figure 4. Impact of velocity profile at various Gm values.

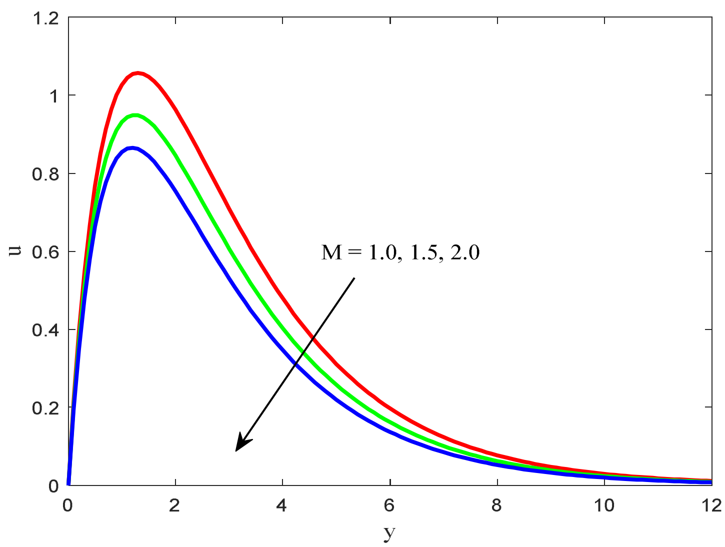

Figure 5. Impact of velocity profile at various M values.

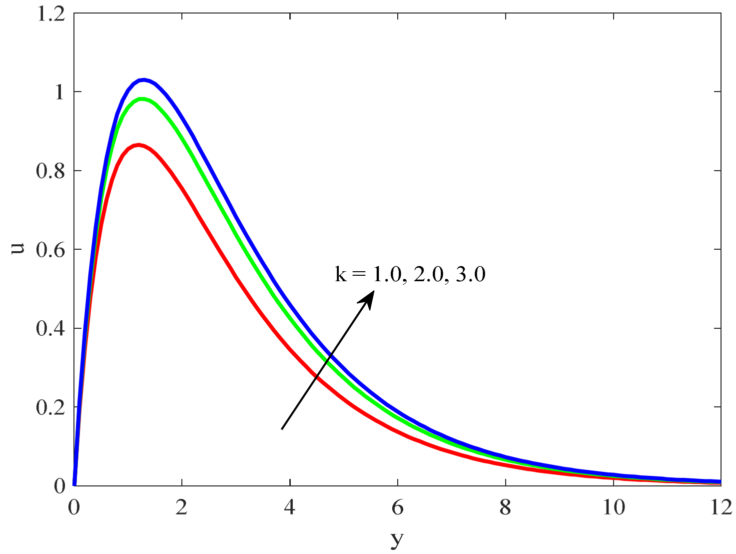

Figure 6. Impact of velocity profile at various K values.

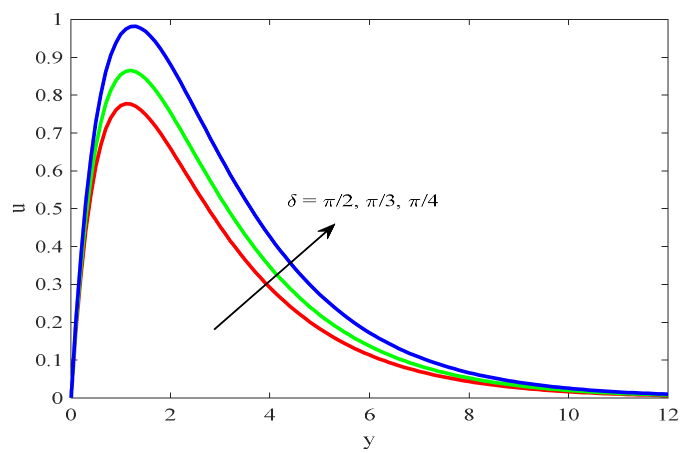

Figure 7. Impact of velocity profile at various δ values.

Figures (8) through (10) of the findings display the thermal profiles. When the fluid in the boundary layer on the surface of the vertical plate is heated, the absorption level falls as the various parameters of $\Pr$, F and Q increases. So, K_o and Sc both have greater parameters. On graphs (11)–(12) however, the concentration gradually drops.

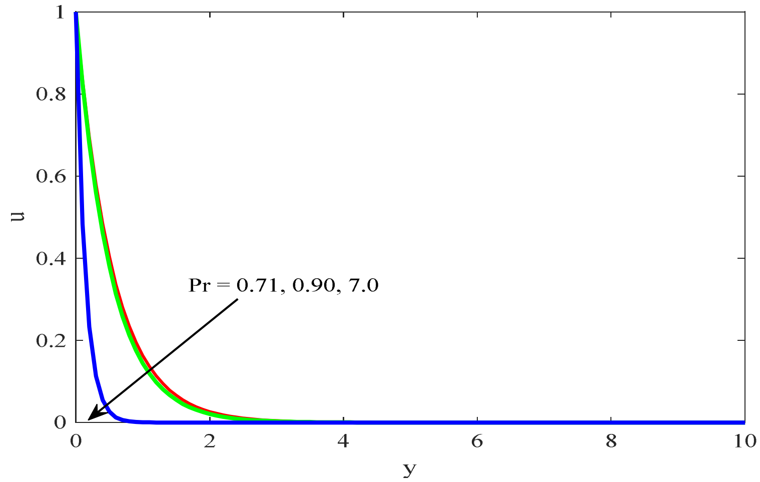

Figure 8. Impact of temperature profile at various $\Pr$ values.

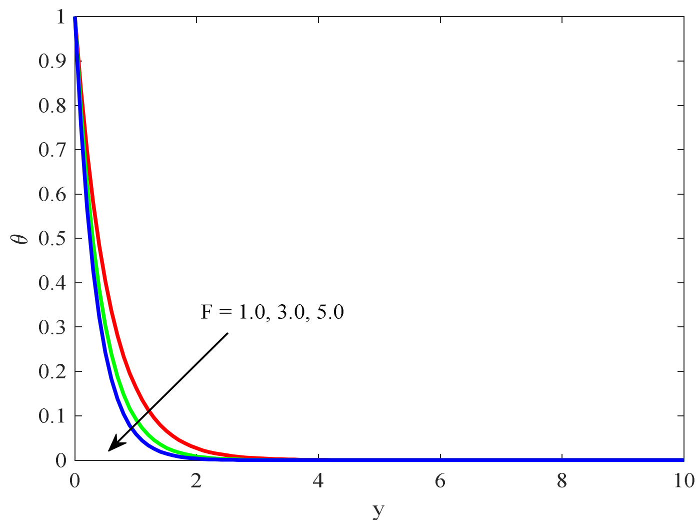

Figure 9. Impact of temperature profile at various F values.

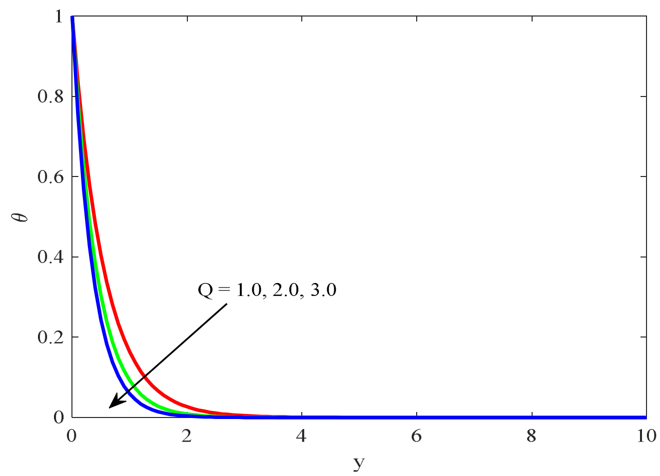

Figure 10. Impact of temperature profile at various Q values.

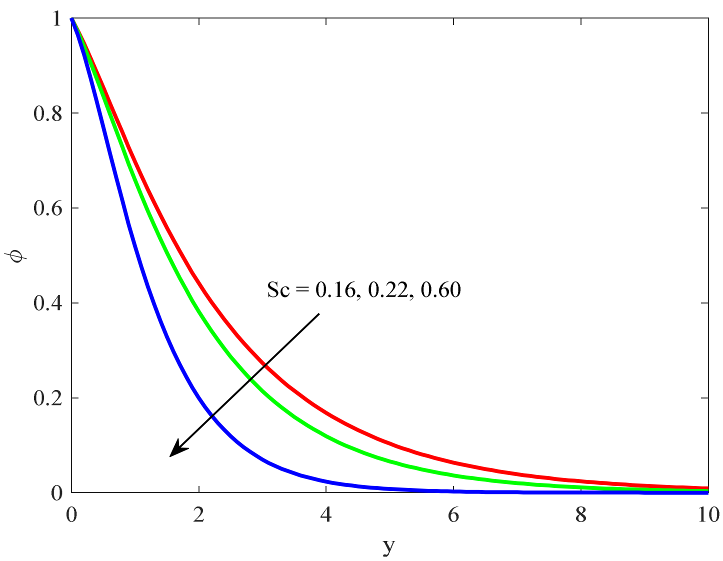

Figure 11. Impact of temperature profile at various Sc values.

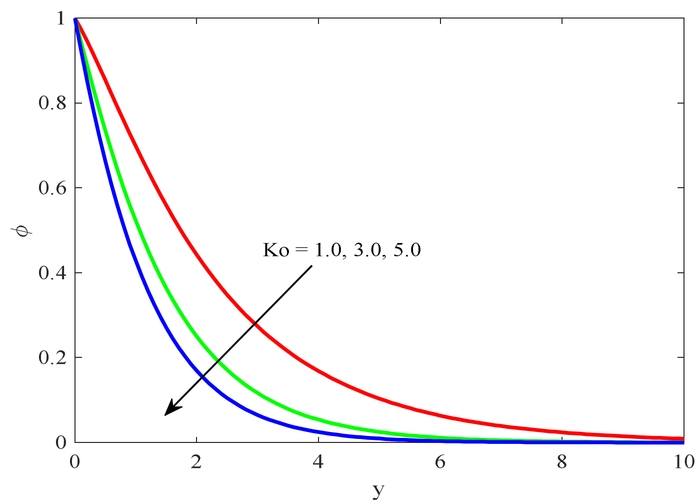

Figure 12. Impact of temperature profile at various K_o values.

Using skin friction coefficients, Table-1 shows the velocity profiles. The Grashof number (Gr) is used for heat transmission. The mass transfer coefficient (Gm) increases when the Casson parameter (γ), the permeability parameter (K) and the magnetic parameter (M) are taken into consideration. Under the Self Profiles in Table-2, the Nusselt number, heat absorption parameter (Q) and Radiation Parameter (F) are shown. The accurate numerical results achieved with the perturbation technique are most clearly shown in Table-2, when compared to the preceding analytical results by Obulesu Mopuri et al. [19].

Table 1. The Skin friction properties by Obulesu Mopuri et al. [19] the Gm, M, K values were compared with the present values in all studies.

Gm	M	K	Obulesu Mopuri et al. [19]	Present Result
5			5.6751	5.5625
10			10.2210	10.4916
15			14.7317	14.4207
	2		5.6751	5.5625
	3		4.9709	4.9619
	4		4.4962	4.4614
		2	6.2316	6.2126
		3	6.4633	6.3846
		4	6.5907	6.4966

Table 2. The Nusselt number F and Q values are compared with the values in the studies by Obulesu Mopuri et al. [19].

F	Q	Obulesu Mopuri et al. [19]	Present Result
4		6.7311	6.6533
6		7.0466	7.0465

	3	6.5589	6.5311
	5	6.8932	6.8720
	6	7.0466	7.0475

6. Conclusion

In this study, convection in a porous media that absorbs Casson fluid flow yields the perfect solutions for the aligned angle and radiation in an infinite vertical plate. The partial differential equation is used analytically in a closed form perturbation technique to graph the effects of velocity, temperature and concentration on the profiles.

Below are some noteworthy findings.

- The absorption velocity on the plate increases in tandem with the increases in Gr, Gm, K and δ. The liquid's absorption velocity fall as γ and M parameters rise.
- The temperature of the heated liquid in the vertical plate falls with an increase in P, F and Q.
- As Sc and K_o values increase, concentration correspondingly falls.
- In Table-1, the skin friction coefficient results for the parameters Gm, M and K are compared to the current result.
- Table -2 compares the recent Nusselt number result with F and Q results.

REFERENCES

[1] Harikrushna M, Prabhakara Rao G, Mallikarjuna Reddy A. Chemical reaction effects on magnetohydrodynamic convective flow past a vertical absorbent plate with ramped wall temperature and concentration. Journal of Wiley Online Library, 2023; 52(6); 3914-35. https://doi.org/10.1002/htj.22856.

[2] Ramalingeswara Rao S, Vidyasagar G, Deekshitulu G V S R. Unsteady MHD free convection Casson fluid flow past an exponentially accelerated infinite vertical porous plate through porous medium in the presence of radiation absorption with heat generation/absorption. Journal of Science of Direct, 2021; 42 (3);1608-16. https://doi.org/10.1016/j.matpr.2020.07.554.

[3] Salahuddin T, Zoehib Mahmood , Mair Khan , Muhammad Awais. A permeable squeezed flow analysis of Maxwell fluid near a sensor surface with radiation and chemical reaction. Journal of Science of Direct, 2022; 562; 111627. https://doi.org/10.1016/j.chemphys.2022.111627.

[4] Kodi Raghunath, Nagesh Gulle, Ramachandra Reddy Vaddemani, Obulesu Mopuri. Unsteady MHD fluid flow past an inclined vertical porous plate in the presence of chemical reaction with aligned magnetic field, radiation, and Soret effects. Journal of Science of Direct, 2022; 51(3); 2742-2760. https://doi.org/10.1002/htj.22423.

[5] Subhrajit Sarma, Sarmand Nazibuddin Ahmed. Thermal diffusion effect on unsteady MHD free convective flow past a semi-infinite exponentially accelerated vertical plate in a porous medium. Canadian Journal of Physics, 2022; 100 (10). https://doi.org/10.1139/cjp-2021-0361.

[6] Hussain Shaik,Venkata Krishna Reddy Bommireddy, Sam Prasanthi Lam, Kalyan Kumar Palaparthi. Radiation Absorption and Diffusion Thermo Effects on Unsteady MHD Kuvshinski Fluid Flow Past an Inclined Porous Plate in the Presence of Thermal Radiation and Chemical Reaction. Journal of Advanced Research in Fluid Mechanics and Thermal Sciences, 2023; 109(1); 162-176. 10.37934/arfmts.109.1.162176.

[7] Anil Kumar Janga, RadhaGajjala. Heat and Mass Transfer on Unsteady MHD Kuvshinski Fluid Flow Past an Inclined Porous Plate with Multiple Slip Effect. Journal of advanced research in Fluid Mechanics and Thermal Sciences, 2023; 106 (2). https://doi.org/10.37934/arfmts.106.2.103115.

[8] Neeraja Gopalam, Saila Kumari Annareddy. Thermal Diffusion and Diffusion Thermo Effects on MHD 3D Mixed Upper Convective Flow of Maxwell Nanofluid Flow Past using Nonlinear Radiative Heat Flux. Journal of CFD Letters, 2023; 15(9); https://doi.org/10.37934/cfdl.13.9.152165

[9] Kodi Raghunath, Mopuri Obulesub, Konduru Venkateswara Raju. Radiation absorption on MHD free conduction flow through porous medium over an unbounded vertical plate with heat source. International Journal of Ambient Energy, 2023; 44(1); 1712-20.

[10] Iskandar Waini, Nurul Amira Zainal, Najiyah Safwa Khashi'ie. Aligned Magnetic Field Effects on Flow and Heat Transfer of the Upper-Convected Maxwell Fluid over a Stretching/Shrinking Sheet. Journal of MATEC Web of Conferences, 2017; 97(3);01078.

[11] Selvaraj, Jothi E. Heat source impact on MHD and radiation absorption fluid flow past an exponentially accelerated vertical plate with exponentially variable temperature and mass diffusion through a porous medium. Journal of Science of Direct, 2021;46 (9); 3490-94.

[12] Raghunath Kodi, Charankumar Ganteda, Abhishek Dasore M,Logesh Kumar G, Laxmaiah, MohdAbul Hasan, Saiful Islam, Abdul Razak. Influence of MHD mixed convection flow for Maxwell nanofluid through a vertical cone with porous material in the existence of variable heat conductivity and diffusion. Journal of science direct, 2023; 44.

[13] Rajdeep Bordoloi, Kalyan Chamuah, Nazibuddin Ahmed. Free Convective MHD Radiative Flow Past a Porous Vertical Plate in a Porous Medium with Chemical Reaction. Journal of Bio interface Research in Applied chemistry, 2023; 13(3) ;2069 – 5837, https://doi.org/10.33263/BRIAC133.259.

[14] Mohana Ramana R ,Venkateswara Raju K, Raghunath K, Chemical reaction with aligned magnetic field effects on unsteady MHD Kuvshinski fluid flow past an inclined porous plate in the presence of radiation and Soret effects. Journal of wiley, 2022; 51(7); 6431-49. https://doi.org/10.1002/htj.22598.

[15] Shankar Goud B, Dharmendar Reddy Y. Chemical reaction and Soret effect on a unsteady MHD heat and mass transfer fluid flow along an infinite vertical plate with radiation and heat absorption. Journal of the Indian Chemical Society, 2022;99(11);100762. https://doi.org/10.1016/j.jics.2022.100762.

[16] Obulesu Mopuri, Raghunath Kodi, Madhu, Mohan Reddy Peram, Charankumar Ganteda, Giulio Lorenzini , Nor AzwadiSidik. Unsteady MHD on Convective Flow of a Newtonian Fluid Past an Inclined Plate in Presence of Chemical Reaction with Radiation Absorption and Dufour Effects. Journal of CFD Letters, 2022; 14 (7); https://doi.org/10.37934/cfdl.14.7.6276.

[17] Srinivasa Rao D, David Kumar R, Sridhar W. Radiation effect on slip flow regime transient MHD fluid in the presence of chemical reaction and soret effect. International Journal of Interdisciplinary Research and Innovations, 2020; 8(1); 42-55.

[18] Raju M C, Madhusudhana Rao, Reddy G V. Thermal radiation and heat transfer effects on steady MHD fluid flow past a vertical porous plate with injection. European Journal of Scientific Research, 2017; 145(1); 112 – 119.

[19] Obulesu Mopuri, Charankumar Ganteda, Bhagyashree Mahanta, Giulio Lorenzini. MHD Heat and Mass Transfer Steady flow of a convective fluid through a porous plate in the presence of multiple parameters. Journal of Advanced Research in Fluid Mechanics and Thermal Sciences, 2022; 89(2); 56-75.

[20] Kamalesh K. Pandit. Unsteady MHD Casson Fluid Flow past an Accelerated Vertical Plate Through Porous Medium in Presence of Thermal Radiation. Journal of Indian Society for Heat and Mass Transfer, 971-981.10.1615/IHMTC-2017.1350.

[21] Asma Khalid, Ilyas Khan, Sharidan Shafie. Exact Solutions for Unsteady Free Convection Flow of Casson Fluid over an Oscillating Vertical Plate with Constant Wall Temperature. Journal of Hindawi, 2015.

[22] Mythreye A, Pramod J P. Effects of Chemical Reaction on Unsteady MHD Free Convective Flows past a Vertical Porous Plate Embedded in a Porous Medium with Variable Suction. European Modern Studies Journal, 2023; 7(4); 10.59573/emsj.7(4).2023.29

[23] Sambaran Pramanik. Casson fluid flow and heat transfer past an exponentially porous stretching surface in presence of thermal radiation. Ain Shams Engineering Journal, 2013; 5(1); 205–212.10.1016/j.asej.2013.05.003.

[24] Hymavathi Talla, Fatima K. Magnetic Field Influence on Radiative Casson Fluid Flow over an Exponetial Stretching Surface. Journal of Pharmaceutical Negative Results, 2022; 13(6); 10.47750/pnr.2022.13.S06.247.

[25] Sridhar W, Ganesh G R, Appa Rao B V, Haile Gorfie E. Mixed Convection Boundary Layer Flow of MHD Casson Fluid on an Upwards Stretching Sheet Encapsulated in a Porous Medium with Slip Effects. JP Journal of Heat and Mass Transfer, 2021; 22(2); 133-149.10.17654/HM022020133.

[26] Hymavathi Talla, PavanaKumari, Sridhar W. Analysis of Flow of a MHD Casson Fluid over an exponentially stretching sheet. International Journal of Management, Technology and Engineering, 2018; 8(9); 740.

[27] Mehari Fentahun Endalew**,** Subharthi Sarkar. Modelling and Analysis of Unsteady Casson Fluid Flow due to an Exponentially Accelerating Plate with Thermal and Solutal Convective Boundary Conditions. Journal of Applied Mathematics, 2023.

[28] Khadijah, Abualnaja M. Implementation of DTM as a numerical study for the Casson fluid flow past an exponentially variable stretching sheet with thermal radiation. International Journal of Modern Physics, 2021; 32(08).

[29] Raghunath Kodi, Obulesu Mopuri, Sujatha Sree, Venkateswaraju Konduru. Investigation of MHD Casson fluid flow past a vertical porous plate under the influence of thermal diffusion and chemical reaction. Journal of Wiley Heat Transfer , 2021; 1–18.

[30] Ravikumar D, Jayarami Reddy K, Raju M C. Unsteady MHD Thermal Diffusive and Radiative Fluid Flow Past a Vertical Porous Plate with Chemical Reaction in Slip Flow Regime. International Journal of Applied Mechanics and Engineering, 2019; 24(1); 117-129.